Eur. Phys. J. B **41**, 43–48 (2004)
DOI: 10.1140/epjb/e2004-00291-9

THE EUROPEAN PHYSICAL JOURNAL B

On-line monitoring of Au nanoparticles formation by optical spectroscopy

R. Salvati[1], A. Longo[1], G. Carotenuto[1], L. Nicolais[1], S. De Nicola[2], and G.P. Pepe[3,a]

[1] Istituto per I Materiali Compositi e Biomedici – Consiglio Nazionale delle Ricerche, Piazzale Tecchio 80, 80125 Naples, Italy
[2] Istituto di Cibernetica – Consiglio Nazionale delle Ricerche " E Caianiello", Via Campi Flegrei 34, 80078-Pozzuoli, Italy
[3] Coherentia INFM – Università di Napoli "Federico II" – Dipartimento Scienze Fisiche, Fac. Ingegneria, P.le Tecchio 80, 80125 Napoli, Italy

Received 7 April 2004 / Received in final form 13 July 2004
Published online 30 September 2004 –

Abstract. Experimental results concerning the synthesis of gold nanoparticles prepared by alcoholic reduction of Au(III) ions in presence of a polymeric stabilizer, and UV-visible spectroscopic characterization is presented. Optical spectroscopic data have been correlated to *off-line* size measurements obtained analysing transmission electron micrographs. The gold cluster size, coming from both TEM micrographs and absorbance cubic root, behaved linearly with time above a threshold temperature (70 °C) according to a deposition-controlled growth mechanism. The plasmon peak halfwidth behaved linearly with inverse particle radius (obtained by TEM), thus proving the hypothesized mechanism growth. The spectroscopic approach allows an *on-line* gold cluster measurement with possibility to fine control particle size also in the case of a fast process.

PACS. 73.20.Mf Collective excitations (including excitons, polarons, plasmons and other charge-density excitations) – 78.67.Bf Nanocrystals and nanoparticles

1 Introduction

Metal clusters play an important role in many different technological areas. For example, they can serve as model systems to experimentally probe the effects of quantum confinement on electronic, magnetic, and other properties. They have also been widely exploited for use in photography, catalysis, biological labeling, photonics, optoelectronics, information storage, surface enhanced Raman scattering (SERS), formulation of magnetic ferrofluids, etc. [1,2]. The intrinsic properties of a nano-structured metal are mainly determined by its size, shape, composition, crystallinity, and structure. In principle, accurate control of any one of these parameters allows for fine tuning of the properties of nano-structured material-based devices. Currently, the use of metal clusters as advanced additives for plastics functionalization is attracting more and more attention and considerable research activities are being done in this novel field of composite science [3,4]. Because of surface effects and the dramatic changes in properties occurring when the critical length governing some physical phenomenon (magnetic, structural, etc.) becomes comparable with size, metal clusters present unique properties (e.g., near-IR photoluminescence, superparamagnetism, plasmon absorption, etc.). The embedding of nanoscopic metal structures into polymeric matrices represents the most simple way to protect clusters and to take advantage of their physical characteristics. Polymer-embedded gold nanoparticles have been frequently investigated [4].

Because of their unique physical characteristics, gold/polymer nanocomposites are potentially useful for a number of advanced functional applications, especially in the field of optics and photonics. In particular, these materials can be used as light-stable color filters [5], polarizers [6,7], ultra-low refractive index materials [8], nonlinear optical devices [9], optical sensors [10], etc.

Polymer-embedded metal clusters can be obtained by using two different approaches, which can be classified as in situ and ex situ. In the in situ methods, metal clusters are generated inside a polymer matrix by decomposition (e.g., thermolysis, photolysis, radiolysis, etc.) or chemical reduction of a metallic precursor dissolved into the polymer. In the ex situ approach, clusters are first produced by soft-chemistry routes and then dispersed into polymeric matrices.

Since the performance of a nanostructured material depends on its physical properties, which are related to a variety of structural factors (size, shape or composition), *on-line* in situ morphological monitoring techniques plays a role of primary importance. When the nanoscopic objects to be prepared consist of nano-sized metals

[a] e-mail: gpepe@na.infn.it

characterized by a surface plasmon absorption (i.e., collective oscillations of conduction electrons at metal surface), the use of real-time UV-Vis-NIR spectroscopy represents an efficient in situ monitoring method. In order to verify the validity of such approach, gold nanoparticles have been prepared by a typical synthetic route (that is, alcoholic reduction of Au(III) ions in presence of a polymeric stabilizer), and the average size of resulting gold clusters has been measured *off-line* by Transmission Electron Microscopy (TEM) at different reaction times. The temporal evolution of the absorption spectra have been recorded during the reaction and the absorbance peak properties has been correlated to the particle size. The comparison between UV-Vis and TEM data confirmed that the measurements methods are consistent, and can be indifferently employed for the determination of the particle size. The *on-line* in situ optical spectroscopy technique allowed also to determine that a surface-deposition controlled kinetic was the predominant mechanism governing the particle growth rate in the reactive mixture. Section 2 describes the chemical synthesis, and the experimental results in terms of structural, morphological and optical properties. Section 3 reports data concerning optical absorption spectra in the 190–1200 nm wavelength range for different reaction temperatures and times. Analysis of experimental data is developed in Section 4 where evidence of the correlation between TEM results and UV-visible spectroscopic data is also presented.

2 Experimental

Metallic nanopowders were obtained by alcoholic reduction of metallic ions in presence of a polymeric stabilizer [11,12]. The precursor used to synthesize gold clusters was the tetrachloroauric acid ($HAuCl_4{\cdot}3H_2O$ 99.9%, Aldrich). Due to the hygroscopic nature, this compound was stored in a dry-seal vacuum desiccator. Ethylene glycol ($C_2H_6O_2$ 99%, Aldrich) was employed both as solvent and reducing agent of tetrachloroauric acid. Poly(N-vinyl pyrrolidone) (PVP, Aldrich, $M_w = 10,000$ a.m.u.), previously dried in oven at 40 °C for two hours, was the protective agent. Au-PVP samples were separated and washed by acetone (C_3H_6O 99.9%, Aldrich). All reagents were used without further purification.

The method for gold clusters preparation involved the mixing under stirring of two different solutions. In particular, the first of these two solutions was obtained by dissolving 5 g of poly(N-vinyl pyrrolidone) into 15 g of ethylene glycol. In order to obtain reproducible results this solution had to be aged for at least 48 hours at room temperature [13,14]. The second solution was freshly prepared by dissolving 12.5 mg of tetrachloroauric acid into 6 ml of ethylene glycol at room temperature. These solutions were mixed and the reaction was isothermally carried out.

The reaction progress was monitored by *off-line* and *on-line* techniques using TEM and UV-Visible spectroscopy respectively.

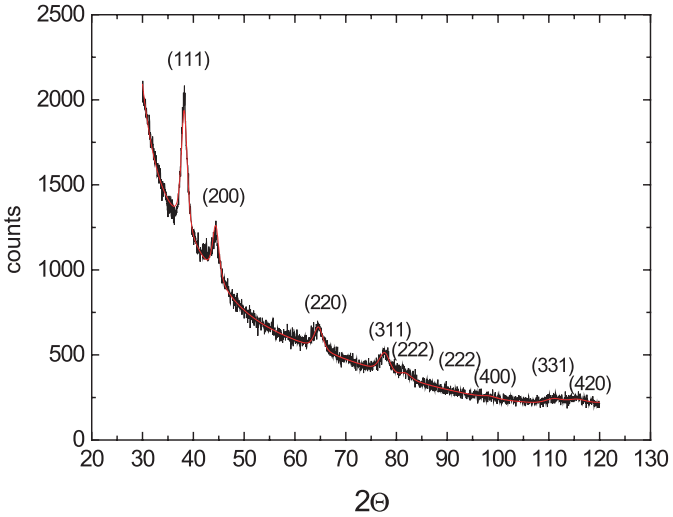

Fig. 1. XRD of PVP-embedded gold nanoparticles (T = 80 °C, t = 65 s). The Bragg peaks of fcc gold are labeled. The bottom of the figure displays the residual of a fit based on the Rietveld method.

In order to stop the reaction and to separate nanoparticles, for X-ray diffraction and TEM characterization, the reactive mixture was cast into a large amount of acetone (250 ml) and the system was sonicated for several minutes. Au-PVP nanocomposite system was achieved after flocculation. The product was washed several times with acetone and then dried at room temperature under vacuum.

For UV-Visible characterization, the above mentioned procedure was not required. In fact, the reaction development was entirely monitored, in *real-time*, by using a spectrophotometer and a computer for spectroscopic data recording.

Morphological and structural characterization was obtained by X-ray diffraction (XRD) and TEM analysis. XRD measurements were performed with a Rigaku DMAX-IIIC goniometer using Cu-K_α radiation (λ = 0.154056 nm) and a pyrolytic graphite monochromator in the diffracted beam. The goniometer operate in the standard Bragg-Brentano $\theta/2\theta$ parafocusing geometry.

The XRD profile for the synthesized nanocomposite is reported in Figure 1. The typical pattern of face centered cubic (fcc) gold lattice is superposed to the background signal of the amorphous PVP matrix. The obtained lattice parameter of 4.077(2) Å is in good agreement with the value 4.079 Å reported in the literature (Power Diffraction Data, 4-784) within the limit of the experimental error. This result shows that the nanoparticles were not subjected to a net dilatation or contraction, that might result for instance from size effects or interstitial impurities. The average crystallite size derived from peak broadening analysis was found to be 7 ± 1 nm, quite close to the diameter of the same nanoparticle sample derived by TEM micrographs as discussed below. This result indicates that most nanoparticles are single-crystals.

TEM micrographs were obtained by a Philips EM208S microscope equipped by a MegaView Camera for digital imaging, using an accelerating voltage of 100 kV. In

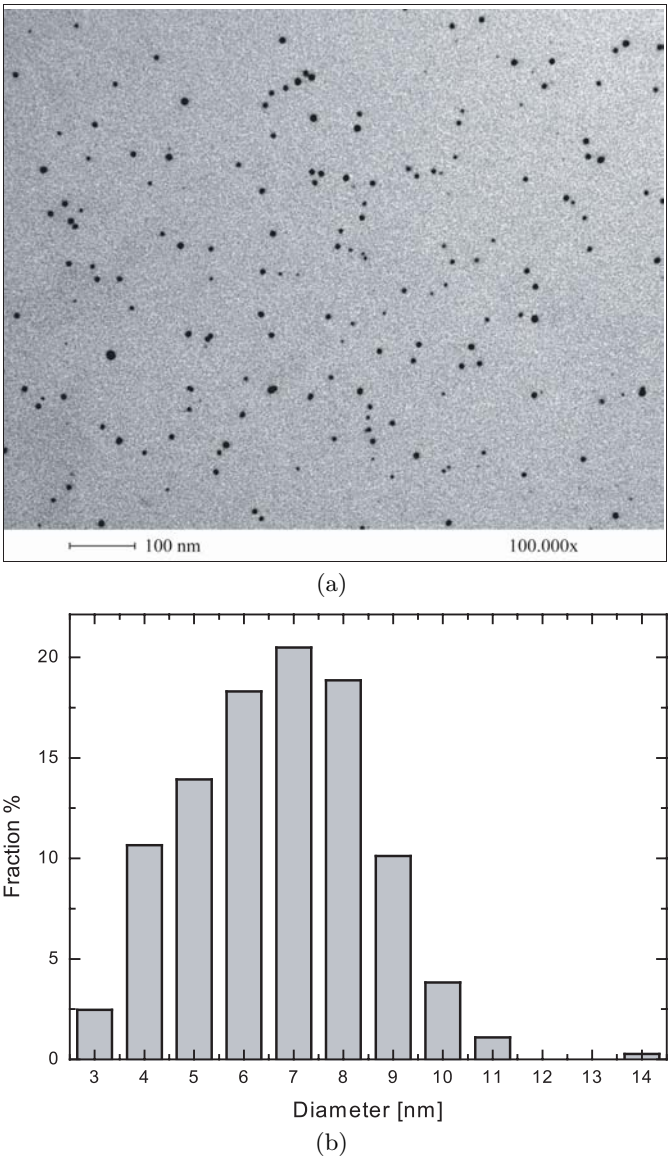

Fig. 2. (a) TEM-micrograph and (b) histogram of PVP-embedded gold nanoparticles obtained at temperature of 80 °C and reaction time of 65 seconds.

the TEM sample preparation Au-clusters/PVP nanocomposites were dissolved in ethanol and the solution cast on graphitized Formovar film supported on copper mesh grids. Digital TEM micrographs have been processed by an image analysis software (Sigma Scan Pro 5) in order to evaluate the particle size distribution. Micrograph analysis were carried out on samples obtained at a reaction temperature of 80 °C ± 0.1 °C for increasing reaction times: 37, 50, 65, 80, 100 seconds. Aggregated systems were not present, while the shape was found to be almost spherical, and the size distribution was very broad. A typical TEM micrograph for the Au-clusters/PVP sample (at reaction time of 65 seconds) and the corresponding histogram distribution are shown in Figure 2. Table 1 provides size distribution parameters.

Table 1. Size distribution parameters for different samples from TEM analysis.

Sampling time	$\langle D \rangle$ [nm]	σ_R[nm]
37 s	3.6	1.3
50 s	5.9	0.9
65 s	6.7	0.8
80 s	7.7	0.9
100 s	11.8	1.7

The formation-growth of gold clusters was monitored by UV-Visible spectroscopy, looking at the very intensive surface plasmon absorption resonance which characterized the nanosized gold particles [15,16].

Absorption spectra were obtained at regular time intervals by using an UV-Visible spectrophotometer (HP-8453 UV-Vis spectrophotometer), which was equipped with a Peltier apparatus to control the reaction temperature (0 to 100 °C with an accuracy of ±0.1 °C), in addition the system employed a magnetic stirrer.

Absorption spectra were monitored and recorded on a personal computer connected to the spectrophotometer.

Since the reaction rate increases with increasing temperature, shorter sampling times were required at higher temperatures; for example at 25 °C the sampling time was 120 s, whereas at 100 °C it was only 0.5 s. Typical UV-Visible spectra obtained at 80 °C and at two reaction times, namely 37 s and 65 s, are shown in Figures 3a, b respectively.

The behaviour of recorded UV-visible spectra is produced by three main factors: (i) the absorption produced by the Au^{3+} ions, (ii) the $5d \rightarrow 6sp$ interband transition of gold clusters, and (iii) the surface plasmon absorption band of gold clusters. Three Lorentzian functions corresponding to the mentioned contributions were used for peak deconvolution. They are visible in Figures 3a, b at two different reaction times (37 s and 65 s), while the continuous line represents convolution function. The negative peak which corresponds to the reduction of the Au^{3+} ions during the reaction, becomes much less evident when the other two contributions are predominant. Such a behaviour is in agreement with leaching of yellow colour of gold ion solution visible at reaction beginning. Lorentzian deconvolution of the spectral data allows for accurate determination of the physical characteristics of plasmon peak, i.e. the maximum wavelength, the full width at half maximum (FWHM), the integral area under the absorbance curve, etc. Such deconvolution gives only approximate results since susceptibility (and not absorption constants) are additives.

In the following section the way to measure from optical data is discussed in addition to hypothesis on the cluster grow mechanism.

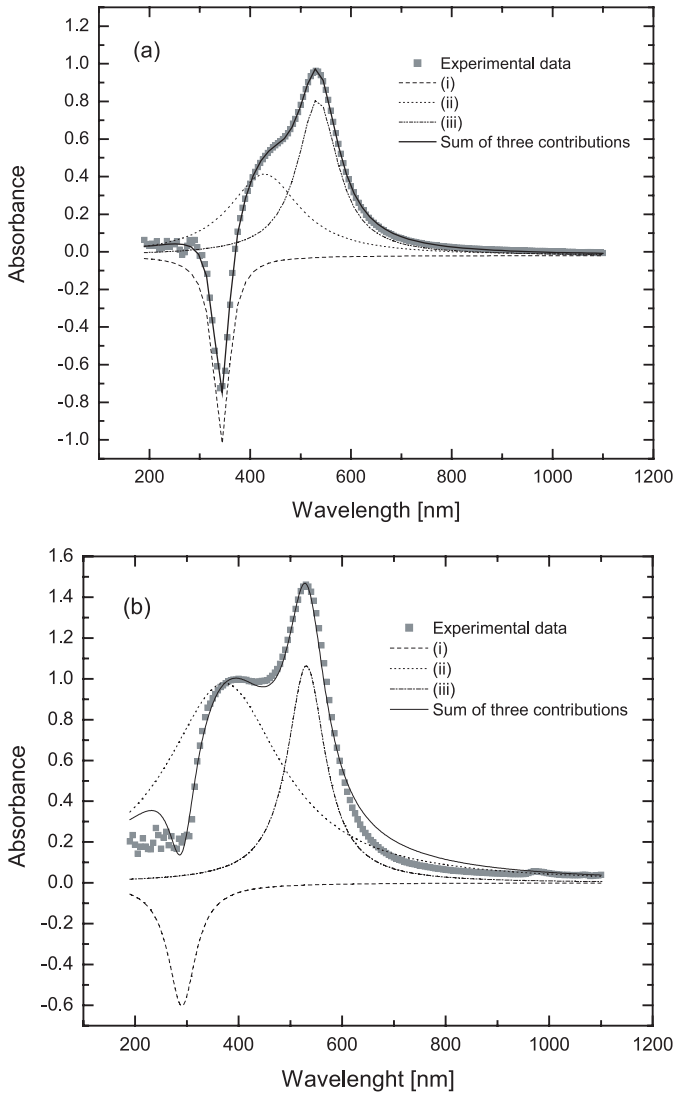

Fig. 3. UV-visible spectrum of a gold mixture corresponding to a reaction time of (a): 37 s and (b): 65 s. Curves represent the deconvolution results obtained form the experimental absorbance: dash, dot, and dash-dot lines correspond to effects (i), (ii), (iii) as described in the text. The solid line is the sum of dashed curves.

3 Results and discussion

The analysis of the plasmon absorption peak provides information on the size of the growing nanoparticles. Well-established theoretical models [17] allows to correlate the optical absorption spectra both to the morphological and topological structure of nano-particle systems dispersed into a homogeneous dielectric medium. Peak position, shape, FWHM, maximum value of the absorption spectrum are related to the shape, diameter and composition of clusters system. In the investigated samples, analysis of the plasmon peak resonance, performed through a deconvolution of the absorbance spectra, suggests that gold particles are mainly spherical in shape, and contact-free. The particle formation-growth mechanisms can be established too. Indeed, the theory [17] predicts that the optical absorption A is dependent on the number N and the size R of the cluster, and this dependence is governed by simple scaling law, $A \propto NR^3$, where N and R change continuously during the reaction time. Nucleation process increases the number N and different particle size growth mechanisms affects differently the size R of the gold cluster. Therefore, the behaviour of the cubic root of the measured absorbance vs. the reaction time t can be considered a finger print of the dominant mechanism contributing to the particle growth [18].

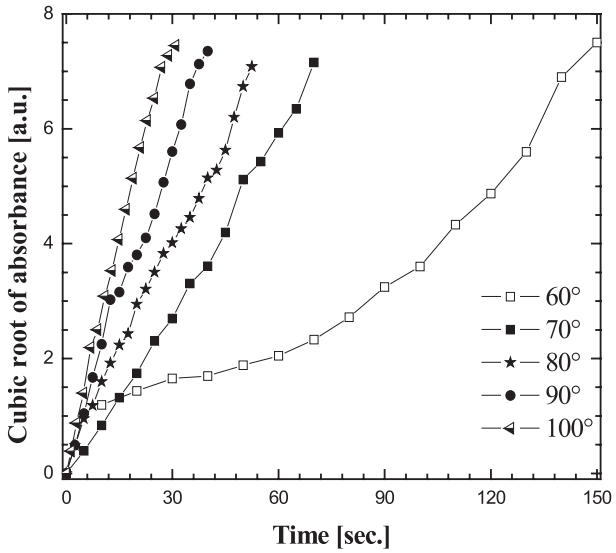

Fig. 4. Time dependence of the cubic root of the absorbance at different reaction temperatures.

A quantitative analysis of optical spectra in terms of cluster dimension can be performed under the hypothesis that the number N of the clusters in the solution does not change during the reaction. This happens when the nucleation rate is high enough that the nucleation stage and the growth stage are separated. In other words, in this condition all cluster nuclei can be assumed to be generated at same time with a subsequent common growth stage. If the temperature is high enough, the produced clusters have approximately the same dimensions, that is, the sample is monodispersed [18,19].

In these conditions the cubic root of absorbance vs. reaction time can be directly related to the size increase of clusters. Two different kinetic mechanisms of particle growth-rate come into play: diffusion-controlled and deposition-controlled. The predominant kinetic effects depends essentially on which of these two mechanism is the slowest one. Under diffusion-controlled kinetic, the temporal evolution of growth rate of the cluster radius scales as $\sqrt{t}$, the square root of the reaction time, whereas, in the case of a deposition-controlled kinetics is linear in t [18]. Data shown in Figure 4 clearly suggest that the predominant mechanism is the deposition-controlled at reaction temperatures higher than 70 °C. The line between the experimental data points is a guide for the eye.

At temperatures below 70 °C a s-shaped curve behaviour of the cubic root of the absorbance vs. time curves

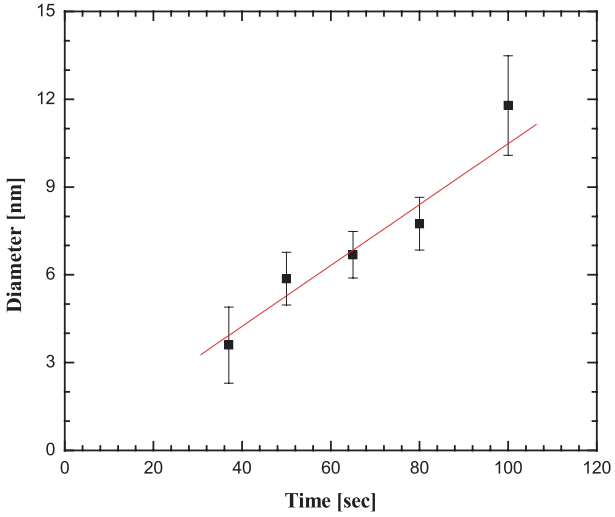

Fig. 5. Nanoparticles averaged diameter as measured by TEM vs. reaction time for a sample obtained at temperature $T = 80$ °C.

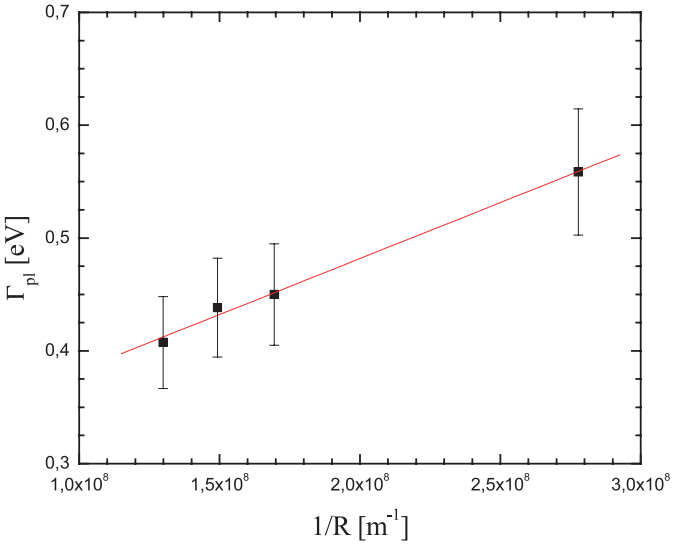

Fig. 6. Halfwidth of the plasmon peak ($\Gamma_{\rm Pl}$) as a function of the inverse of the average particle size.

Table 2. UV absorption data.

Sampling time	$\hbar\varpi_{\rm Pl}$ [eV]	$\Gamma_{\rm Pl}$ [eV]	$\hbar\varpi_{\rm ib}$ [eV]	$\Gamma_{\rm ib}$ [eV]
37 s	2.31	0.56	2.98	1.00
50 s	2.32	0.45	3.03	1.62
65 s	2.32	0.44	3.28	2.05
80 s	2.33	0.41	3.15	1.45

can be clearly discerned from the experimental data. This behaviour can be related to a continuous formation of new nuclei during the reaction [20]. In this condition the cubic root of absorbance cannot be directly related to the size of the clusters, and hence it is possible to ascertain which kinetic growth mechanism is now predominant. The crossover temperature between these two regimes depends on the initial gold precursor concentration. At lower concentrations of gold ions, the reaction rate is slower and the formation and growth of the clusters is very easy in this condition.

On the other hand, TEM analyses demonstrated that the average size of nanoparticles grows linearly with the reaction time (see Fig. 5). This behaviour is also a fingerprint of the surface-deposition controlled kinetic mechanism.

Similar behaviours have been also reported for gold cluster formation in formaldehyde-based systems [21].

Table 2 summarizes the main physical characteristics of the UV spectra in terms of plasmon energy ($\hbar\omega_{\rm Pl}$), plasmon halfwidth ($\Gamma_{\rm Pl}$), interband energy peak ($\hbar\omega_{\rm ib}$), interband transition halfwidth ($\Gamma_{\rm ib}$). The relationship between the plasmon peak characteristics and the effective nanoparticle size, as measured by TEM micrographs, can be used for an *on-line* control of the average nanoparticle radius. In particular, the linear dependence of the $\Gamma_{\rm Pl}$ as a function of the inverse of the average particle size R, as shown in Figure 6, is in agreement with that expected from theory [17]. The value of the slope in the $\Gamma_{\rm pl}$ vs. $1/R$ curve is 1×10^{-9} eVm, and it is in quite good agreement with the theoretical value obtained by Mie theory in the case of spherical gold nanoparticles, i.e. $\hbar v_{\rm F} g(\nu) = 3.033 \times 10^{-9}$ eVm, where $\hbar$ is the Planck constant, $v_{\rm F}({\rm Au}) = 1.04 \times 10^6$ ms^{-1} the Fermi velocity, and $g(\nu) = 4.419$, where $\nu = \hbar\omega_{\rm pl}/E_{\rm F}({\rm Au}) = 0.422$ is a function defined in reference [22].

The intersection of the $\Gamma_{\rm pl}$-curve with the ordinate, by extrapolating down to the limit $1/R \to 0$, gives a size independent contribution of about 0.27 eV. Neglecting radiation damping, this value is related to $\Gamma_{\rm ib}$, and hence it is expected to be larger in the case of gold nanoparticles with respect the case of Ag clusters, because of a stronger contribution from interband transitions in Au nanoparticles [23]. On the other hand, no appreciable dependence on the particle radius R is observed for the measured energies of the plasmon peak as shown in Table 2. This analysis demonstrates the possibility that an in situ spectroscopy-based approach, which measures the plasmon peak and its halfwidth, can be efficiently employed both for monitoring and controlling the nanoparticle size growth during the chemical synthesis.

Conclusions

The size control of metal nanoparticles constitutes a crucial aspect of the synthesis process, since little changes of the particle diameter may led to dramatic changes both in the physical and chemical properties. In the case of nano-sized metals characterized by surface plasmon absorption, optical spectroscopy represents a valid approach for the in situ *on-line* size monitoring. By applying this technique to gold nanoparticles prepared by alcoholic reduction of Au(III) ions in presence of a polymeric stabilizer, UV absorption spectra recorded during the reaction

at temperatures where the growth is deposition-controlled, have been correlated to *off-line* TEM photographs. This analysis has confirmed the assumption that the growth mechanism (deposition-controlled mechanism) shows the same linear dependence in both cubic root absorbance and average particle radius vs. reaction time. Moreover, the complete agreement between the plasmon halfwidth as a function of the inverse of the particle radius further confirms the relation between the optical in situ data and the particle size determined by TEM. This method allows to measure indirectly in *real-time* the size of the nanoparticles during their growth without the need to stop the reaction. In addition, this approach allows for fast and accurate identification of nanometric solid-phase formation and sizing. The short sampling times possible with the spectrophotometer approach allows to study the mechanism of fast reactions for the cluster formation.

We would like to tank G. Cafiero and the staff of C.I.S.M.E of the University of Naples "Federico II" for their assistance in TEM analysis.

References

1. W. Eberhardt, Surface Science **500**, 242 (2002)
2. R.H. Kodamo, J. Magn. Magn. Mater. **200**, 359 (1999)
3. See, for example: a) A.B.R. Mayer, Mater. Sci. Eng. C **6**, 155 (1998); b) W. Scheunemann, H Jaeger, Z. Physik **265**, 441 (1973); c) A. Heilmann, C. Hamann, Prog. Coll. Polym. Sci. **85**, 102 (1991)
4. W. Caseri, Macromol. Rapid Commun. **21**, 705 (2000)
5. A.G. deLeon, Y. Dirix, Y. Staedler, K. Feldman, G. Hahner, W.R. Caseri, P. Smith, Appl. Opt. **39**, 4847 (2001)
6. A.H. Lu, G.H. Lu, A.M. Kessinger, C.A. Foss, J. Phys. Chem B **101**, 9139 (1997)
7. Y. Dirix, C. Darribere, W. Heffels, C. Bastiansen, W. Caseri, P. Smith, Appl. Opt. **38**, 6581 (1999)
8. L. Zimmerman, M. Weibel. W. Caseri, U.W. Suter, P. Walther, Polym. Adv. Technol. **4**, 1 (1993)
9. G.L. Fisher, R.W. Boyd, in *Nanostructured Materials Cluster, Composites, and thin films*, edited by V.M. Shalaev, M. Moskovits (Washington DC, 1998), p. 108
10. R.D. Harris, J.S. Wilkinson, Sensors and Actuators B **29**, 261 (1995)
11. T. Sugimoto, Fine Particles (Marcel Dekker, New York, 2000), Vol. 2
12. P.Y. Silvert, K. Tekaia-Elhsossen, Solid State Ionics **82**, 53 (1995)
13. G. Carotenuto, S. De Nicola, G.P. Pepe, L. Nicolais, Eur. Phys. J. B **24**, 437 (2001)
14. G. Carotenuto, S. De Nicola, L. Nicolais, J. Nanoparticle Res. **3**, 467 (2001)
15. J. Turkevich, G. Garton, P.C. Stevenson, J. Colloid Sci. **9**, 26 (1954)
16. K. Fukumi, A. Chayahara, K. Kadono, T. Sakaguchi, Y. Horino, M. Miya, K. Fujii, J. Hayakawa, M. Satou, J. Appl. Phys. **75**, 3075 (1994)
17. U. Kreibig, M. Vollmer, *Optical Properties of Metal Clusters* (Springer-Verlag, 1995)
18. T. Sugimoto, Monodispersed Nanoparticles (Elsevier, 2001)
19. V.K. LaMer, R.H. Dinegar, J. Amer. Chem. Soc. **72**, 4847 (1950)
20. J. Turkevich, P.C. Stevenson, J. Hillier, Discussion Faraday Soc. **11**, 55 (1951)
21. R. Zsigmondy, E. Hückel, Kolloidchemie **III-IV**, 921 (1925)
22. U. Kreibig, J. Phys. F: Metal Phis. **4**, 999 (1974)
23. L. Genzel, T.P. Martin, U. Kreibig, Z. Physik B **21**, 339 (1975)